

# A Stretchable and Tough Small-Scale Magnetic Actuator for Biomedical Applications

Joseph Berbner<sup>1</sup> and Ron Dennis<sup>#</sup>

<sup>1</sup>Wellington College, Crowthorne, Berkshire, UK

<sup>#</sup>Advisor

## ABSTRACT

A stretchable, tough, small-scale magnetic actuator capable of multimodal locomotion under magnetic fields is proposed. The actuator consists of a silicone elastomer (Ecoflex 00-10) embedded with neodymium-iron-boron (NdFeB) particles and coated with a poly(2-methacryloyloxyethyl phosphorylcholine) (PMPC) triple network hydrogel layer. The hydrogel layer is biocompatible and decreases the surface friction of the actuator. Mechanically, the actuator is highly stretchable, tough, and fatigue-resistant. The application of the actuator in drug delivery is demonstrated.

## **Introduction**

Nature endows microorganisms with mechanical properties and sensing capabilities that readily allow them to respond to different environments. Such high functionality and autonomy has prompted research into synthetic materials that can adapt to external stimuli because of their importance in biomedical applications. In particular, adaptable small-scale actuators find use in biosensing [1], minimally invasive surgery, and drug delivery [2]. Such actuators can respond to a wide array of stimuli including light [3], temperature [4] and electric fields [5]. A particularly promising option for biomedical applications is using magnetic fields as an external stimuli. This is because magnetic fields are safe and able to penetrate many materials. Magnetic stimulation and ferromagnetism have been the most common methods for actuation in soft magnetic robots. In magnetic stimulation, magnetic particles are incorporated into a material and a magnetic field is applied in order to actuate the material. This allows the fabrication of robots with high degrees of freedom, endowing them with the ability to jump, swim, and transport small cargo [6]. However, the biocompatibility and mechanical reliability of existing magnetic robots remains questionable. In this work, a tough, highly stretchable, and biocompatible magnetic actuator capable of multimodal locomotion under magnetic fields is developed. We use a silicone elastomer (Ecoflex 00-10) embedded with neodymium-iron-boron (NdFeB) magnetic particles as the matrix for the robot. The magnetic particles are used to prescribe a magnetization profile for the actuator. We further apply a poly(2-methacryloyloxyethyl phosphorylcholine) (PMPC) triple network hydrogel coating on the surface. PMPC triple networks are biocompatible, tough, and increase surface lubrication [7]. The hydrogel coating makes the actuator biocompatible and decreases its surface friction. Under the presence of a magnetic field, the magnetic particles align in the direction of the field, which allows for multimodal locomotion of the actuator [8]. By controlling the direction of the magnetic field, the actuator can deform into different configurations, potentially allowing it to jump, swim, and transport small cargo (Figure 1).

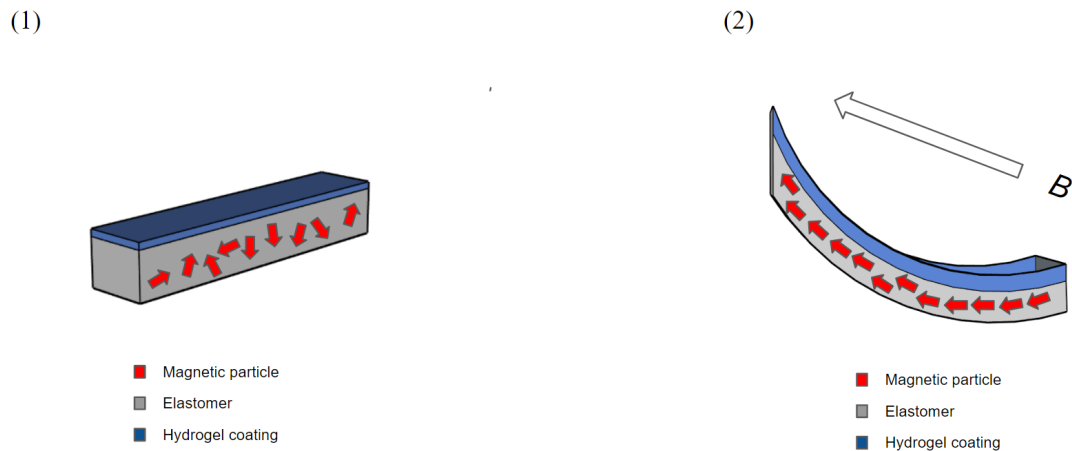


**Figure 1.** The actuator consists of a silicone elastomer (Ecoflex 00-10) embedded with neodymium-iron-boron (NdFeB) particles and coated with a poly(2-methacryloyloxyethyl phosphorylcholine) (PMPC) triple network hydrogel layer. **Figure 2.** Under the presence of an external magnetic field  $B$ , the magnetic domains align in the direction of the field allowing the actuator to deform.

## Material Model and Mechanical Properties

In describing the mechanical properties of our actuator, we assume that the presence of the particles and the hydrogel coating influence the bulk behavior of the actuator negligibly. The effect of the particles on the stiffness of the actuator has already been studied [6] where it is shown that a 75% increase in particle concentration leads to a less than 10% increase in material stiffness. The mechanical behavior of silicone elastomers is well characterized by the Neo-Hookean model, with a stiffness of 0.02 MPa [10]. We thus adapt the Neo-Hookean model and characterize the behavior of our actuator. The free energy,  $W$  of the Neo-Hookean model is given by:

$$W = \mu/2 (\lambda_1^2 + \lambda_2^2 + \lambda_3^2) \quad (1)$$

where  $\mu$  is the shear modulus, and  $\lambda_1, \lambda_2, \lambda_3$  are the stretches in each principal direction. We model our actuator as an incompressible material such that  $\lambda_1 \lambda_2 \lambda_3 = 1$ . For an incompressible material, the stress can be calculated as:

$$\sigma_1 - \sigma_3 = \lambda_1 \partial W / \partial \lambda_1 \quad (2)$$

We use two representative tests to characterize our material: uniaxial tension and pure shear. The former is chosen because it is the simplest and most standard laboratory test to characterize the mechanical properties of a material. The latter is chosen because it is the most common test to quantify the toughness of a material. Under uniaxial tension, a sample is clamped on one end and pulled on the opposite end. As a stress,  $\sigma$ , is applied, the sample elongates from a length,  $L$  to a new length,  $l$ , as shown in Figure 2(a). Note that the material shrinks in the lateral direction due to Poisson's effect. In pure shear, a sample with a width much larger than its height is clamped on one end as shown in Figure 3(a). As a stress,  $\sigma$ , is applied, the sample elongates from a length,  $L$  to a new length,  $l$ , (Figure 3(b)).

(3)



(4)

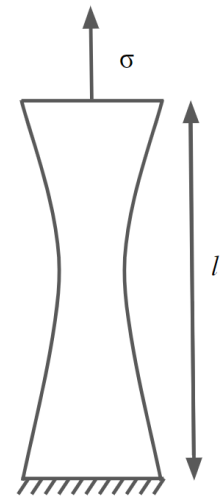


**Figure 3.** In the reference state, a sample of length  $L$  is fixed at the bottom end. **Figure 4.** In the deformed state, a stress  $\sigma$  is applied, and the sample is deformed to a new length  $l$ , and the sample shrinks laterally.

(5)



(6)

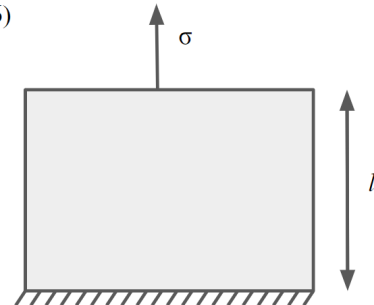


**Figure 5.** In the reference state, a sample with width much greater than its length,  $L$  is fixed at the bottom end. **Figure 6.** In the deformed state a stress,  $\sigma$  is applied. It is assumed that no deformation occurs horizontally, and the new length of the sample is  $l$ .

Note that unlike in uniaxial tension, the sample does not deform in the lateral direction. This assumption is made since the sample width is much larger than the sample height. In both tests, we define the stretch of the sample as  $\lambda=l/L$ . Under uniaxial tension, the stress-stretch relationship is of the form

$$\sigma = \mu(\lambda^2 - 1/\lambda)$$

where  $\mu$  is the shear modulus Under pure shear, the stress-stretch relationship is of the form:

$$\sigma = \mu(\lambda^2 - 1/\lambda^2).$$

Figure 7 plots the stress as a function of stretch under for both uniaxial tension and pure shear. The figure demonstrates that the material behaves similarly under both uniaxial tension and pure shear conditions. The behavior is nonlinear, and the material begins to stiffen around a stretch of 2.5. Figure 8 plots the initial

portion of stress as a function of stretch for both uniaxial tension and pure shear. The behavior is linear, and it is seen that the material is stiffer under uniaxial tension.

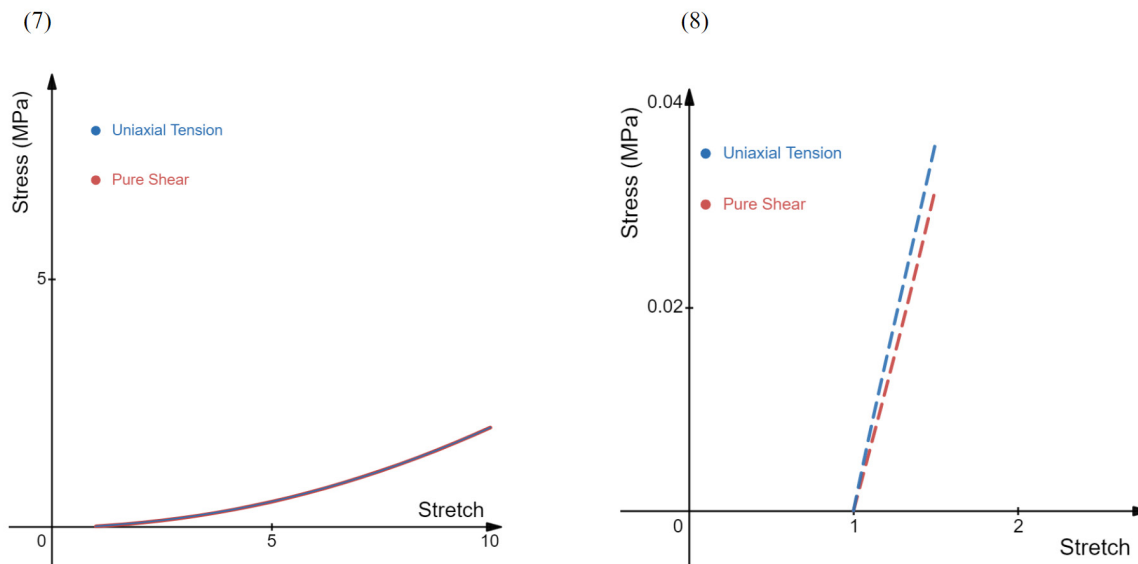


**Figure 7.** Stress-stretch curve of elastomer under uniaxial tension and pure shear. **Figure 8.** Initial portion of the stress-stretch curve of the elastomer under uniaxial tension and pure shear

We next use a combination of experimental data and our material model to estimate the toughness of our sample. The toughness of a silicon elastomer of similar composition in pure shear was measured to be 3.58 KJ/m<sup>2</sup> [11]. From the provided stress-stretch plots, we estimate their modulus to be 0.25 MPa. Toughness in pure shear is calculated as  $WH$ , where  $W$  is the strain energy density of the sample at rupture and  $H$  is the height of the sample. Adopting the Neo-Hookean model, the toughness is given by:  $\Gamma = \mu/2 (\lambda_b^2 + 1/\lambda_b^2 - 2)H$ , where  $\lambda_b$  is the stretch at break. Thus, for  $\Gamma = 3.58$  kJ/m<sup>2</sup> and  $\mu = 0.25$  MPa, the breaking stretch is  $\lambda_b = 2$ . Assuming our material breaks at a similar breaking stretch for a pure shear configuration of the same height, its toughness is given by  $\Gamma = 0.25/2 (2^2 + 1/2^2 - 2)15 \sim 4.2$  kJ/m<sup>2</sup>, which is on the same order of natural tissue found in the human body. For example, the toughness of cartilage is around 1kJ/m<sup>2</sup> [12]. Thus, our actuator is tough enough to be used for most biological applications.

## Hydrogel coating

We next add a thin, biocompatible hydrogel coating to decrease the surface friction of our actuator. We choose a poly(2-methacryloyloxyethylphosphorylcholine) (PMPC) triple network (TN) hydrogel for our coating. The hydrogel's triple network structure greatly reduces its wear and friction while maintaining excellent mechanical properties. For instance, the coefficient of friction of such a network is reported to be less than 0.08 while its yield stress is 26 MPa [7]. Note that although traditional double network hydrogels demonstrate adequate frictional properties, their biological applications are hindered because of their tendency to wear [13]. Indeed, a double network hydrogel achieves a low friction coefficient solely by inducing a biphasic lubrication phase. This is in contrast to naturally wear-resistant materials which achieve low friction through a combination of both biphasic lubrication and boundary lubrication. However, double network hydrogels lack the boundary lubrication that is present in naturally wear-resistant materials—such as cartilage. The addition of a third PMPC network endows the hydrogel with a boundary lubricating phase in addition to the already present biphasic

lubrication. The resulting hydrogel's frictional properties closely resemble that of cartilage, making it suitable for biological applications. In particular, we hypothesize that the exceptionally low friction coefficient and low tendency to wear will allow the actuator to travel freely in the human body while inducing negligible shear stresses on surrounding surfaces. The synthesis of the triple PMPC network will closely resemble the process used in [7], with a minor modification: the first network will be synthesized with 2 mol% MBAA instead of 4 mol%. The synthesis procedures of the second and third networks will be unmodified. The change in crosslinker concentration in the first network is done to reduce the stiffness of the hydrogel, while leaving its toughness and frictional properties unchanged. Although the stiffness of the hydrogel in [7] was not reported, we have estimated the stiffness from the stress-strain curves to be around 0.2 MPa, which is an order of magnitude higher than the stiffness of silicon rubber. Hence, to ensure stiffness compatibility within the actuator it is suggested that half the crosslinker density is used to synthesize the first network of the PMPC hydrogel. The hydrogel will be adhered to the elastomer by treating the elastomer with 10 wt.% benzophenone in ethanol solution [14].

## Drug Delivery

Due to the ability to readily prescribe a magnetization profile in the actuator and the safety of magnetic fields in the human body, the proposed actuator can be a promising alternative to current methods of drug delivery. For instance, a magnetization profile can first be programmed. An external magnetic field can then be applied to allow the actuator to pick up the drug.

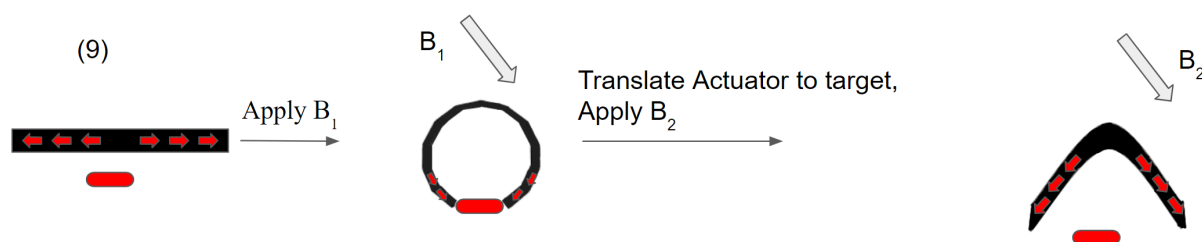


**Figure 9.** An external magnetic field is applied allowing our actuator to pick up the drug.

The actuator can then translate to the intended target and an opposing magnetic field can be applied to allow the actuator to deliver the drug (Figure 9). Unlike previous works, the actuator's surface has low friction and is biocompatible, making it ideal to transport objects in the human body.

## Conclusion

In this work, we have developed a biocompatible magnetic robot with excellent mechanical properties that is capable of multimodal locomotion under the presence of magnetic fields. A material model that governs the behavior of the robot is presented and its applications in drug delivery is demonstrated. Future work is needed to assess the biocompatibility of the robot in vivo.

## Acknowledgments

**I would like to thank my advisor for the guidance provided to me on this project.**

## References

- [1] Ceylan H, Giltinan J, Kozielski K, Sitti M. Mobile microrobots for bioengineering applications. *Lab on a Chip*. 2017;17(10):1705-1724. doi:10.1039/c7lc00064b.
- [2] Sitti M, Ceylan H, Hu W, et al. Biomedical applications of Untethered Mobile Milli/Microrobots. *Proceedings of the IEEE*. 2015;103(2):205-224. doi:10.1109/jproc.2014.2385105.
- [3] Guan L, Yang Y, Jia F, Gao G. Highly transparent and stretchable hydrogels with rapidly responsive photochromic performance for UV-irradiated optical display devices. *Reactive and Functional Polymers*. 2019;138:88-95. doi:10.1016/j.reactfunctpolym.2019.03.003
- [4] Dong L, Agarwal AK, Beebe DJ, Jiang H. Adaptive liquid microlenses activated by stimuli-responsive hydrogels. *Nature*. 2006;442(7102):551-554. doi:10.1038/nature05024
- [5] Han D, Farino C, Yang C, et al. Soft Robotic Manipulation and Locomotion with a 3D Printed Electroactive Hydrogel. *ACS Appl Mater Interfaces*. 2018;10(21):17512-17518.
- [6] Hu W, Lum GZ, Mastrangeli M, Sitti M. Small-scale soft-bodied robot with multimodal locomotion. *Nature*. 2018;554(7690):81-85. doi:10.1038/nature25443
- [7] Milner PE, Parkes M, Puetzer JL, et al. A low friction, biphasic and boundary lubricating hydrogel for cartilage replacement. *Acta Biomaterialia*. 2018;65:102-111. doi:10.1016/j.actbio.2017.11.002
- [8] Kim Y, Yuk H, Zhao R, Chester SA, Zhao X. Printing ferromagnetic domains for untethered fast-transforming soft materials. *Nature*. 2018 Jun;558(7709):274-279. doi: 10.1038/s41586-018-0185-0. Epub 2018 Jun 13. PMID: 29899476.
- [9] Fusco, Stefano, et al. "Shape-switching microrobots for medical applications: The influence of shape in drug delivery and locomotion." *ACS applied materials & interfaces* 7.12 (2015): 6803-6811
- [10] Marechal L, Balland P, Lindenroth L, Petrou F, Kontovounisios C, Bello F. Toward a Common Framework and Database of Materials for Soft Robotics. *Soft Robot*. 2021 Jun;8(3):284-297. doi: 10.1089/soro.2019.0115. Epub 2020 Jun 24. PMID: 32589507.
- [11] Ahmad D, Sahu SK, Patra K. Fracture toughness, hysteresis and stretchability of dielectric elastomers under equibiaxial and biaxial loading. *Polymer Testing*. 2019;79:106038. doi:10.1016/j.polymertesting.2019.106038
- [12] Simha NK, Carlson CS, Lewis JL. Evaluation of fracture toughness of cartilage by micropenetration. *Journal of Materials Science: Materials in Medicine*. 2004;15(5):631-639. doi:10.1023/b:jmsm.0000026104.30607.c7
- [13] Simha NK, Carlson CS, Lewis JL. Evaluation of fracture toughness of cartilage by micropenetration. *Journal of Materials Science: Materials in Medicine*. 2004;15(5):631-639. doi:10.1023/b:jmsm.0000026104.30607.c7
- [14] Yuk, H., Zhang, T., Parada, G. A., Liu, X., & Zhao, X. (2016). Skin-inspired hydrogel-elastomer hybrids with robust interfaces and functional microstructures. *Nature Communications*, 7(1). <https://doi.org/10.1038/ncomms12028>

